

Generation of Microstructural Gradients for Improved Mechanical Properties via Thermo-Hydrogen Treatment of the Metastable Beta Titanium Alloys Beta CTM and Ti 10V-2Fe-3Al

Christopher David Schmidt, Vitali Macin, Peter Schmidt and Hans-Jürgen Christ,
Institut für Werkstofftechnik, Universität Siegen, Germany

Structural components must be lightweight and produced resource-saving while still fulfil the increasing durability and reliability requirements. One approach to fulfil these requests is a temporary hydrogen charging of Ti-alloys, which generates lattice distortion and hydrides. The volume difference between hydride precipitates and the alloy matrix results in localized plastic deformation. This triggers recrystallization and enables a finer microstructure as attainable by a conventional heat treatment. The study aims at an elaboration of a thermo-hydrogen treatment that establishes a change in grain size and/or an alteration in distribution and morphology of strengthening secondary α precipitates as a function of the distance to surface (microstructural gradient). The gradient is based on a gradient of the hydride volume fraction. Generally, THT design requires kinetic (temperature dependency of the hydrogen diffusion coefficient D_H) in addition to thermodynamic (H/ β -Ti-alloy interaction) data, which has been obtained for Ti 3Al-8V-6Cr-4Mo-4Zr and Ti 10V-2Fe-3Al. Subsequent to a solution treatment the variation of hydrogenation time and temperature is operated to establish comparably slight microstructural gradients on these materials. For further investigations it is concluded that materials with less alloying elements ((α + β)-Ti-alloys (e.g., Ti 6Al-4V)) than these β -Ti-alloys can satisfy the requirements to generate steeper microstructural gradients even better.

Introduction

Previous works observed an improved fatigue life of Ti-alloys after a conventional microstructure modification (e.g., mechanical surface treatments [1-2]). Clearly, a suitable change in grain size as well as in distribution and morphology of strengthening precipitates as a function of the distance to surface (DTS), called microstructural gradient, may enhance the mechanical properties at static and cyclic load. Berg proved that a decreasing secondary α (hcp) phase (α_s) volume fraction with increasing DTS elevates the resistance to crack initiation [1]. Additionally, Burghardt [2] provided the evidence that a coarse-lamellar morphology reduces the crack propagation velocity, while Schmidt [3] observed crack closure, evoked by the existence of primary α (α_p , hcp). In general, a hard sample surface area with a ductile core often fulfils the requirements that result in a microstructure with extended crack initiation stage as well as enhanced crack propagation resistance. *Metals that possess a sufficient hydrogen solubility can be processed by means of thermo-hydrogen treatment (THT) and this treatment may be used to establish microstructural gradients.* The resulting mechanical properties are comparable to those after mechanical surface treatments. Certainly, THT can be applied to complex sample geometries [3]. *THT usually consists of solution treatment (ST), diffusion-controlled H-uptake (hydrogenation), degassing and aging. Since the metal-gas reaction is completely reversible, hydrogenation is temporary. The extrinsic effects can be described by two main phenomena. On the one hand, H is a strong β (bcc)-stabilizing element in Ti-alloys. The H uptake reduces the β transus temperature T_β to $T_{\beta(H)}$ leading to a finer microstructure after subsequent heat treatment steps.* On the other hand, H induces lattice distortion and dislocations. Furthermore, H oversaturation causes hydride formation at sufficient hydrogen concentration ($c_H > c_{H_{yd}}$). This results in an increased number of recrystallization nuclei by dislocation accumulation and vacancy generation at hydride dissolution. Additionally, hydride-forming alloying elements are redistributed and can stabilize the α phases. Previous works of THT that were mainly performed on common (α + β)-Ti alloys aimed at homogeneous microstructures and led to an increased strength at cyclic and static loading. Compared to Ti-microstructures, generated in conventional heat treatments, the THT-microstructures of β -Ti-alloys exhibit either a refined α_s -precipitation morphology via the hydride dissolution (Ti 3Al-8V-6Cr-4Mo-4Zr (Beta CTM)) or a hydride-induced deformation that empowers recrystallization, resulting in grain refinement (Ti 10V-2Fe-3Al (Ti 10-2-3)) [3]. The microstructure gradient from THT could be generated via a hydride phase volume fraction gradient resulting during a heat treatment of the alloy with a diffusion-controlled c_H -gradient. The internal hydrogenation (analogously to the well-known internal oxidation process), whereby the penetrating dissolved hydrogen reacts with (H-)affine alloying elements, should result in a spontaneous local hydride formation [4]. This effect can lead to a purely H diffusion-controlled reaction, causing metal-hydride formation [5] and enabling the generation of local areas, that vary in their hydride volume fraction. These areas are confined by the mobile reaction front (before: a lot of hydrides, behind: zero hydrides), that moves from the surface to the center of the sample.

Sozanska elaborated a THT for Ti-6Al-4V (Ti 6-4) including a hydrogenation cycle with various hydrogenation temperatures (T_{Hydro}). This work proved the possibility to create desired microstructural gradients with THT [6]. Schmidt and Macin focused on the determination of the material parameter values of β -Ti alloys that are necessary for the determination of the THT-parameters (T , c_H and t of each step) [3,7]. Here the T - and c_H -dependant phase stability as well as the kinetic data (temperature dependency of the diffusion coefficient D_H) in addition to the H-solubility at constant H partial pressure of Beta CTM and Ti 10V-2Fe-3Al (Ti 10-2-3) were determined. As a by-product of the experiments that aimed for the determination of the phase stability, THT-induced microstructural gradients appeared. A graded hydride phase volume fraction and a β -grain size gradient after hydrogenation led to a grain refinement in the surface area after dehydrogenation [3]. In this study the detailed phase maps (Figure 1) are the basis for the systematic variation of the THT parameters (T , t , c_H).

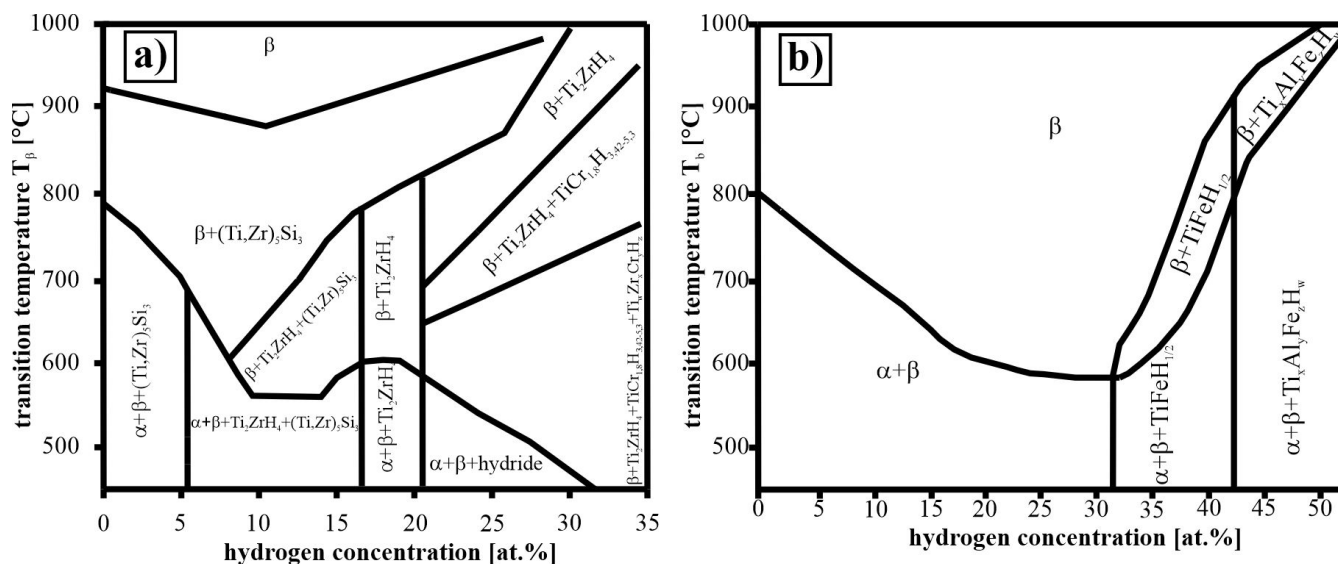


Figure 1: H-influence on phase stability of a) Beta CTM and b) Ti 10-2-3 [7]

Materials and experiments

In this study the first two steps of THT (ST and hydrogenation) were performed on Beta CTM and Ti 10-2-3, since previous works detected the possibility to establish a THT-induced graded microstructures in these materials. The required material characteristics were available from previous studies. Pre-experiments confirmed that a small variation of t and T used for the ST has negligible influence on hydride-induced phase transformation. Hence, the ST parameters from Macin et al. were chosen [7]. The samples (\varnothing 12 mm, 50-100 mm length) were hydrogenated at a hydrogen partial pressure of 100 mbar in a horizontal vacuum furnace with attached He/H₂ gas supply. To inhibit oxidation of the sample surface, the samples were placed on a Zr foil. The selection of the temperature range for the experiments was made in order to ensure a direct hydride precipitation in the β +hydride phase field of Beta-C and the α + β +hydride phase regime of Ti 10-2-3. Therefore, T_{Hydro} was set to 600 and 650°C for Beta CTM leading to $c_{hyd}=13$ at.-% while for Ti 10-2-3 T_{Hydro} was set to 550°C and 600°C resulting in $c_{hyd}=32\%$ at.-%. These comparably low temperatures require a hydrogen absorption catalysis which was realized with a Pd-coating of the samples. The gradients are adjustable by a variation of diffusion time, which is why the hydrogenation experiments of Beta CTM were performed for 1, 2, 4 and 6 h at 600 °C and 650 °C. Ti 10-2-3 was hydrogenated for 1, 2, 4, 6 and 8 h at 550°C and for 1, 2, 3, 4, 5 and 6 h at 600°C. The analysis of the hydrogenated microstructures was carried out by FE SEM to display qualitatively grain size- and volume fraction gradients. The EDS point analyses complemented the investigation in order to quantify the redistribution of alloying elements concomitant to hydrogenation. The value of c_H in the near-surface area was determined with a carrier hot gas extraction.

Results

BetaCTM

First the results of hydrogenation of Beta CTM are represented. Hydrogenation for 1 and 2 h at 600°C results in a negligible change of the microstructure. The 4 h hydrogenation (600°C) leads to a microstructural gradient (Figure 2a) and b)). The white, acicular hydride phase appears exclusively from the edge (Figure 2a)) to a DTS of 1 mm (Figure 2b)). As seen in Figure 2c) the increase of the hydrogenation annealing duration t_{Hydro} to 6 h generates crumbling of the sample. Aside from this phenomenon, hydride formation appears at the grain boundaries of the sample core (Figure 2d)). The hydrides are shaped as needles or plates and form preferentially at dislocation arrangements and at silicides. When T_{Hydro} is changed to 650°C, a 2 h hydrogenation leads to a direct hydride formation within the whole microstructure. After 4 h the distribution of hydrides does not change significantly anymore. A microstructure gradient has been generated after 6 h, meaning that the hydride phase volume fraction decreases with increasing DTS. The high hydride volume fraction in the surface area seems to be responsible for the initiation of surface cracks. In contrast to hydrogenation at 600°C (6 h), at 650°C (6 h) hydrides were formed homogeneously in the core and near the surface of the sample.

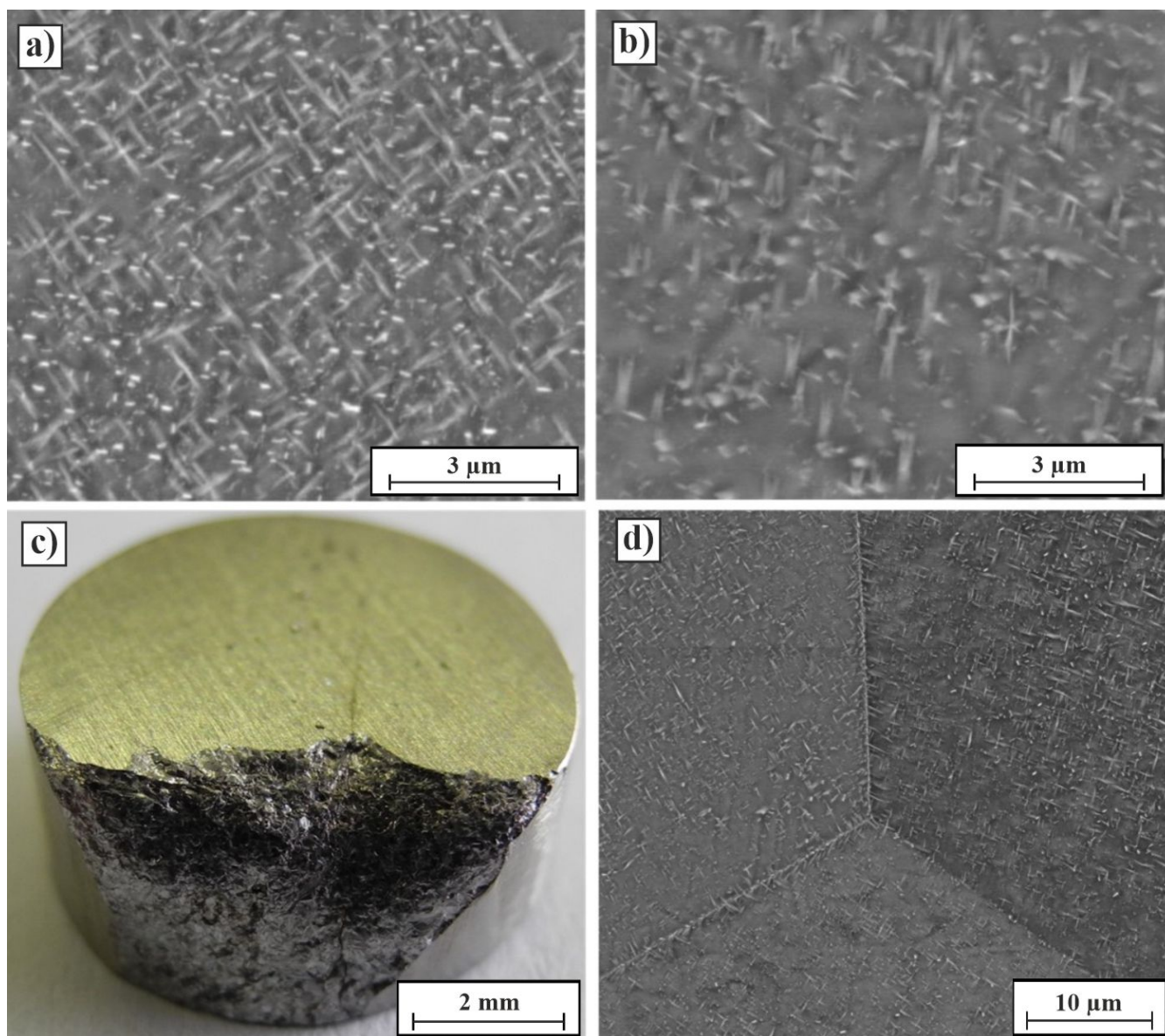


Figure 2: FE-SEM micrograph of Beta-CTM after hydrogenation at 600°C for 4 h ($c_H > 30$ at.-%: a) surface and b) 1 mm DTS), and for 6 h ($c_H > 35$ at.-%: c) destruction of sample at surface and d) undamaged area in the core)

Ti 10-2-3

Hydrogenation of Ti 10-2-3 at 550°C shows results comparable to those of the 600°C hydrogenation. Since the effects of the hydrogenation on the microstructure are more pronounced at 600°C, the results of hydrogenation at 600°C are portrayed exclusively here (see Figure 3). The resulting microstructures exhibit the α_p phase (black equiaxed phase), α_s -precipitates (dark grey needles) and the β -matrix (light grey phase). While the α_p phase and α_s -precipitates occur in the center and the surface area, the microstructure at the core contains martensitic, orthorhombic α'' phase regions (grey areas) that retain from ST. The α'' -free area occurs in the region from surface to 4 mm DTS. A comparison of the microstructures at the surface and in the core proves an α_s -precipitation gradient with increasing volume fraction and particle size at increasing DTS, while α_p is distributed approximately homogeneously.

After 2 h (Figure 3c)) a slight microstructural gradient was observed and the microstructure close to the center consists of α_p phase as well, embedded into the β matrix. The qualitative analysis of the α_p phase volume fraction yields 10-12 vol.-% in the center and 6-8 vol.-% at the near-surface area. The acicular α_s phase that was detected after 1 h, is vanished.

On the contrary, the near-surface region of the microstructure generated by hydrogenating for 3h (Figure 3d)), consists of the β -matrix, the residual α_p phase (see black phase in Figure 3c)) at former α_p/β phase boundaries and β -grains that are streaked with white needles. A close-up of this new phase is depicted in Figure 3e) and is called transformed α_p phase ($\alpha_{p-trans}$ (hcp)) in the following. Although the appearance of $\alpha_{p-trans}$ at BSE-mode is comparable to the original β phase, the chemical compositions diverge significantly. The EDS point analysis of the $\alpha_{p-trans}$ phase (Figure 3f)) and the residual α_p phase (Figure 3g)) reveals an enrichment of Ti (3.64 at.-%) within $\alpha_{p-trans}$ that is realized at the expense of Fe (0.79 at.-%), Al (2.26 at.-%) and V (0,6 at.-%).

Finally, hydrogenation for 6 h was performed, providing a graded hydride phase volume fraction and a slight particle size gradient (Figure 3h + i)). With regard to the surface area (Figure 3h)) and the center of the 6 h-sample (Figure 3i)) Ti-Fe-hydrides (white dots) occur in addition to hydride-free α_p areas (appears black in Figure 3h) and dark grey at Figure 3d)) throughout the entire microstructure. The hydrides are more frequent in the near-surface region and situated at α_p/β phase boundaries (Figure 3h)). A qualitative comparison of Figure 3h) and i) indicates a significant decrease of the hydride phase volume fraction within the microstructure from surface to center, while the size of the hydrides gently increases with increasing DTS. Furthermore, the α_p phase volume fraction slightly decreases with increasing DTS. Moreover, the α_s phase was not detected at all. The resulting microstructures after 4 and 5 h (not depicted) show homogeneously distributed hydrides.

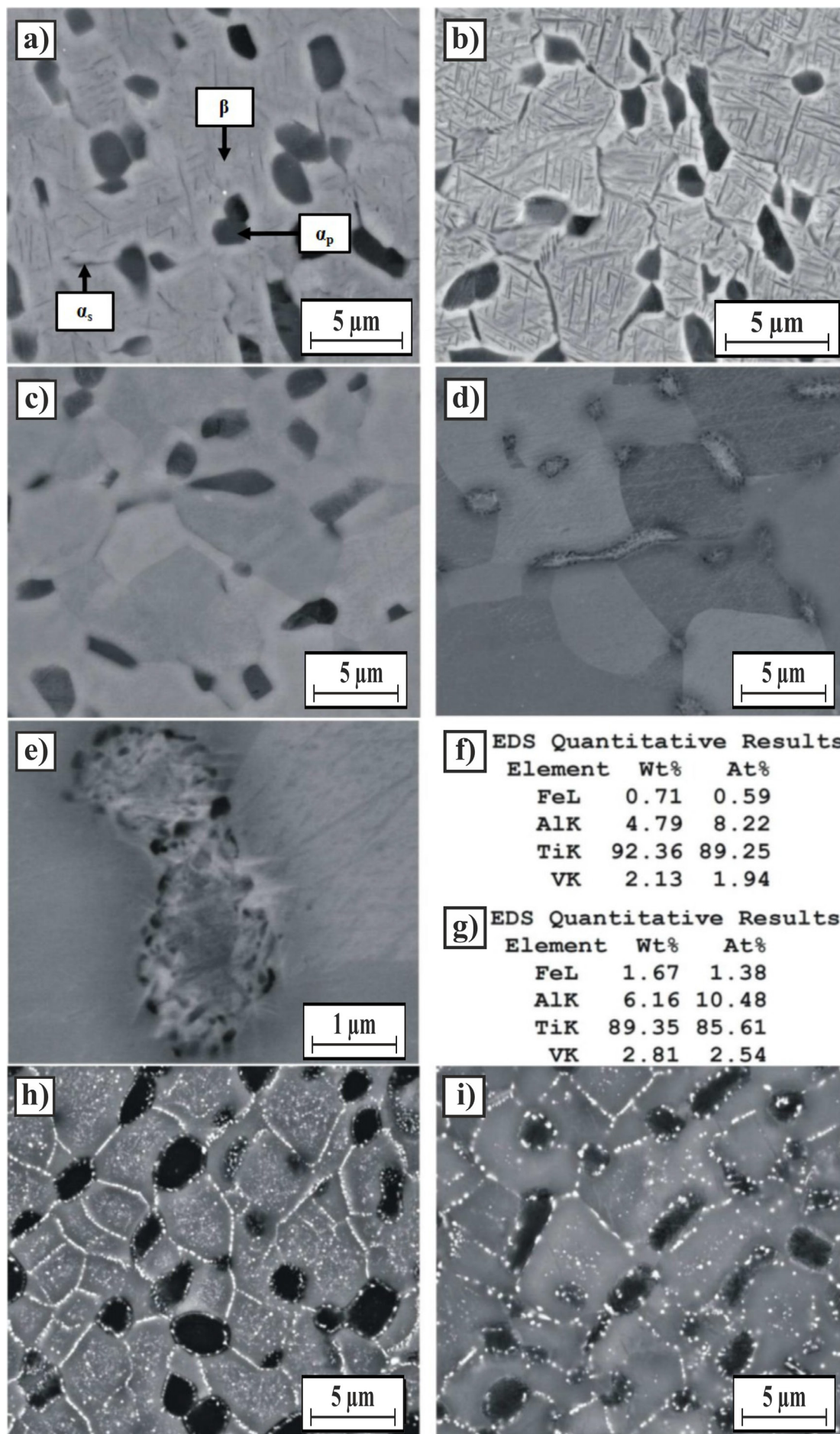


Figure 3: FE-SEM micrographs of the microstructure of Ti 10-2-3 after hydrogenation at 600°C for 1 h: a) surface area and b) center; after hydrogenation at 600°C for c) 2 h (center) and d) 3 h (surface area); e) transformation of α_p after 3 h of hydrogenation at 600°C; f) and g) EDS Quantitative Results.

EDS-point analysis of the transforming α_p and β of the residual α_s ; FE-SEM micrographs after hydrogenation at 600°C for 6 h: h) surface area and i) center

Discussion

Beta CTM

In Beta CTM the generation of a hydride volume fraction gradient can be realized but results in crumbling of the samples. A possible explanation for the initiation of cracks at the used hydrogenation parameters arises from the consideration of the phase diagram in Figure 1a). Hydrogenation with a duration above 3 h leads to the evolution of ternary and quaternary hydride phases, since the H concentration reaches $c_H > 30$ at.-%. At the hydrogenation parameters applied a massive growth of the hydride volume fraction is caused with increasing t_{Hydro} , resulting in surface cracks. The diffusion velocity of H is superior to those of the metallic alloying elements that react with H to form hydrides. A c_H gradient that is desired to evoke a subsequent graded volume fraction of hydride precipitates, may be established but is leveled before hydrides can be formed. Consequently, the metallic diffusion determines the velocity of the process. Since the material systems used in this study allow the formation of ternary and quaternary hydrides, future investigations on the application of THT to produce a microstructural gradient should focus on less complex materials. In order to ensure the formation of binary hydrides and, therefore, to simplify thermodynamics of the hydride formation reaction a promising candidate alloy would be the $\alpha+\beta$ -Ti-alloy Ti 6-4. This should provide thermodynamic conditions enabling that the hydride formation reaction process follows the mechanism of the classical internal oxidation.

Ti 10-2-3

The hydrogenation of Ti 10-2-3 at 600°C for 1 h generated a α_s phase volume fraction (decreasing with increasing DTS) gradient, which is induced by a c_H -gradient (see Figure 3a) + b)). Considering that the α phase exists within the whole cross-section, c_H does not exceed 20 at.-% at the hydrogenation parameters applied (compare Figure 1b)). This can be explained by the α'' -dissolution that starts at the surface, progresses to a depth of 4 mm and is accompanied with a simultaneous $\alpha'' \rightarrow \alpha_s$ phase transformation. The acicular α_s -precipitates are characterized by an increased size in comparison to the originally α'' -precipitates that were observed after ST. Consequently, the α_s -precipitation volume fraction decreases with increasing DTS. After 2 h, the previously adjusted α_s phase volume fraction gradient vanishes for the benefit of a α_p phase volume fraction gradient. This is realized with beginning H-induced α_p destabilization at the grain boundary triple points. Due to the prior $\alpha'' \rightarrow \alpha_s$ phase transformation (1 h) the β matrix experiences a distortion and the subsequent complete α_s phase suppression (2 h). The EDS-analysis delivers a H-induced, partial dissolution of the α_p phase and a concomitant rearrangement of the alloying elements after 3 h of hydrogenation ($c_H < 32$ at.-%). An annealing in the single β phase field after the hydrogenation process would lead to a complete α_p -dissolution, a subsequent homogeneous redistribution of alloying elements and a β -grain growth. A further increase of t_{Hydro} (4 h - 6 h) evokes hydride formation (at 600°C: $c_H > 32$ at.-%, at 550°C and 8 h, even $c_H > 45$ at.-%). Simultaneously the $\alpha_{p-trans}$ phase is reconverted into the α_p phase. As a consequence, the typical appearance of the α_p phase as equiaxed particles at grain boundary triple points is recreated. The reversion itself proceeds as an equalization of the Al concentration differences within the α_p phase, that is stabilized by H-induced β -stabilization causing in Al-repression out of the β phase. Considering the homogeneous distribution of the hydrides after 4 and 5 h, the c_H gradient (after 2 h) is almost eliminated. The formation of a volume fraction gradient of the hydride phase leads to the assumption that further near-core hydrides form after compensation of a c_H -difference between the interstitially dissolved and the hydride-bonded H. The reaction is followed by a Fe and Al diffusion-controlled transformation of the TiFe- into $Ti_xFe_yAl_z$ -hydrides as well as a direct $Ti_xFe_yAl_z$ -hydride formation via nucleation and growth.

Conclusion

Hydrogenation generates c_H -gradients at Beta CTM and Ti 10-2-3. Reaching $c_H > 30$ at.-% at Beta CTM a local direct hydride formation but also destruction of the sample by a hydride-induced volume effect occurs. For Ti 10-2-3 the microstructural gradient is less pronounced than that established in Beta CTM. Nevertheless, the volume fraction of the hydride phase close to the surface ($c_H > 30$ at.-%) does not lead to destruction of the sample. The concomitant mechanisms for the generation of a gradient microstructure in both materials are:

- The H-uptake is dominated by a surface reaction at comparably low temperatures.
- The hydride formation is based on phase-transformation-controlled H/metal reactions with at least two metallic elements. Since the diffusion of the alloying elements to the hydride nucleation sites is slow in comparison to the hydrogen diffusion, the hydride formation process is restrained by velocity of the metal diffusion. Consequently, a hydride phase volume fraction gradient, evoked by a c_H gradient, is inhibited or (partially) leveled before graded hydride formation occurs.
- Hydrogenation leads to the formation of ternary and quaternary hydrides. Hence, the hydride formation does not follow the mechanism of internal oxidation, where binary hydrides are formed and the microstructural gradient's steepness is

confined.

As a conclusion, the future investigations will focus on the alloy Ti 6-4, which provides less complexity of the thermodynamic description and enhances the predictability of the hydride formation reactions. Additionally, the formation of binary hydrides and therefore internal oxidation shall be enabled. First the kinetic material characteristics and the resulting phase maps will be determined. Afterwards the hydrogenation experiments will be built on these results.

References

- [1] Berg, A., doctoral thesis, Institute of metallurgy and materials engineering, University of Cottbus, Germany, 2000.
- [2] Burghardt, B., doctoral thesis, Institute for physical metallurgy, Technical University of Darmstadt, Germany, 2002.
- [3] Schmidt, P., doctoral thesis, Institute for materials engineering, University of Siegen, Germany, 2018.
- [4] Wagner, C., Corrosion Science, 8, 1968, 889-893.
- [5] Bloch, J., and Mintz, M. H., Journal of Alloy and Compounds, 253-254, 1997, 529-541.
- [6] Sozanska, M., Mater Sci Eng, 22, 2011, 1-11.
- [7] Macin, V. and Christ, H.-J., TMS 2016, Annual Meeting, Supplemental Proceedings, Nashville, TN, USA, 2016, 673-684.